Parametric Instability in GEO 600 Interferometer

LIGO-P070039-01-Z

A.G. Gurkovsky and S.P. Vyatchanin[1]

[1] *Faculty of Physics, Moscow State University, Moscow 119992, Russia,*
e-mail: svyatchanin@phys.msu.ru

(Dated: May 3, 2007)

We present analysis of undesirable effect of parametric instability in signal recycled GEO 600 interferometer. The basis for this effect is provided by excitation of additional (Stokes) optical mode, having frequency ω_1, and mirror elastic mode, having frequency ω_m, when the optical energy stored in the main FP cavity mode, having frequency ω_0, exceeds a certain threshold and detuning $\Delta = \omega_0 - \omega_1 - \omega_m$ is small. We dicuss the potential of observing parametric instability and its precursors in GEO 600 interferometer. This approach provides the best option to get familiar with this phenomenon, to develop experimental methods to depress it and to test the effectiveness of these methods in situ.

I. INTRODUCTION

The full scale operational terrestrial interferometric gravitational wave antennae LIGO have sensitivity, expressed in terms of the metric perturbation amplitude, approximately 3 times better than the planned level of $h \simeq 1\times10^{-21}$ [1, 2] in 100 Hz bandwidth (see the current sensitivity curve in [3]). In Advanced LIGO (to be approximately realized in 2012), after improving noise of test masses (mirrors of a 4 km long optical Fabry-Perot (FP) cavities) and increasing the optical power circulating inside the resonator the sensitivity is expected to reach the value of $h \simeq 1\times10^{-22}$ [4, 5]. GEO 600 interferometer has absolute sensitivity less than LIGO, however, regarding to its armlength (1200 m, in LIGO 4 km) and circulating power (also lower than in LIGO) sensitivity of GEO 600 is an impressive one (see [6, 7]). In particular, GEO 600 has participated and continues to participate (with LIGO and others) in scientific run S5 aimed to register gravitational waves. In addition GEO 600 plays an important role as a testing area for different kinds of new technologies to be applied later for LIGO, e.g., the signal recycling configuration, monolitic fused silica suspension, usage of electro-static actuators, first demonstartion of thermal lensing compensation and several others.

The undesirable effect of parametric instability in Fabry-Perot cavity, which may cause a substantial decrease in antennae sensitivity or even antenna malfunction, was examined in [8]. This effect appears above the certain threshold in the optical power W_c circulating in the main mode, when the difference $\omega_0 - \omega_1$ between frequency ω_0 of the main optical mode and frequency ω_1 of the idle (Stokes) mode is close to frequency ω_m of the mirror mechanical degree of freedom. Coupling between these three modes occurs due to ponderomotive pressure of light in the main mode and Stokes mode and the parametric effect of mechanical oscillation on optical modes. Above the critical value of light power W_c the amplitude of mechanical oscillation is also increasing as the optical power in the idle (Stokes) optical mode gets bigger. However, E. D'Ambrosio and W. Kells have shown [9] that if the anti-Stokes mode (with frequency $\omega_{1a} = \omega_0 + \omega_m$) is taken into account in the same single dimensional model, then the effect of parametric instability will be substantially lower or even excluded. In [10–12] an analysis was given based on the model of power and signal recycled LIGO interferometer. It was demonstrated that anti-Stokes mode could not completely suppress the effect of parametric oscillatory instability. As a possible "cure" to avoid the parametric instability it was proposed [13] changing the mirror shape and introducing low noise damping. D. Blair with colleagues proposed an interesting concept of heating test masses in order to vary the curvature radii of mirrors in interferometer and hence to control detuning and decrease the overlapping factor between the optical and acoustic modes [14–16]. Recently, the instability produced by the optical rigidity was observed in direct experiment [17]. The effect of parametric instability was observed by K. Vahala with collaborators for micro scale whispering gallery optical resonators [18, 19].

In this article we present a detail analysis of parametric instability in signal recycled GEO 600 interferometer and show that in spite of lower optical power in GEO 600 as compared with LIGO, the parametric instability in this interferometer can be observed if detuning $\Delta = \omega_0 - \omega_1 - \omega_m$ is small. It can be done by changing the frequency of anti-symmetric optical mode (see definition below) of interferometer through varying the position of signal recycling (SR) mirror. It allows using GEO 600 as a testing area to observe precursors of PI and to work out technology to avoid it.

In section II we derive the parametric instability conditions in GEO 600 interferometer. The results obtained are discussed in section III. The details of calculations are present in Appendix.

II. GEO 600 INTERFEROMETER

We analyze GEO 600 interferometer with signal recycling (SR) and power recycling (PR) mirrors — see Fig. 1 and notations to it. The interferometer is tuned in resonance and no optical power from the carrier passes through SR mirror. The wave E_6 traveling through it is used to detect the signal. Interferometer is pumped through port F_5. We make the following simplifying assumptions:

- Optical losses in all mirrors as well as thermal noises are not taken into account.
- Transparencies of PR and SR mirrors are T_{pr}, T_{sr} correspondingly and the lengthes of both arms are tuned so that symmetric mode is in resonance with the pump.
- The distances between the beam splitter and PR, SR mirrors are short (about several meters) as compared with the total arm length (1.2 km), hence, we consider the phase advance of the waves traveling between these mirrors as a constant and omit its dependence on frequency.

- We assume that optical properties of the arms are identical. (The analysis of PI in LIGO interferometer with non-identical arms are presented in [20].)
- We do not take into account anti-Stokes mode.

A. Initial equations

We denote the mean (constant) amplitude of the main wave (at frequency ω_0) by calligraph upper case letters, and small, time-dependent amplitudes of Stokes and elastic mode by lower case letters. For example, the complex amplitude of F_1 can be written: $F_1 = \mathcal{F}_1 e^{-i\omega_0 t} + f_1 e^{-i\omega_1 t}$, where the mean amplitude $\mathcal{F}_1$ corresponds to the main mode with frequency ω_0 and small field f_1 — to the Stokes mode with mean frequency ω_1. Below we recalculate all constant amplitudes through amplitude $\mathcal{F}_0$ in arms, so that $\mathcal{F}_1 = \mathcal{F}_2 \equiv \mathcal{F}_0$. We normalize amplitudes so that $|\mathcal{F}_0|^2 = W$, where W is optical power circulating in each arm. The displacements of mirrors' surface are denoted by $x_{1,2}$, $y_{1,2}$, y_{pr}, x_{bs} (see Fig. 1) and we introduce slow amplitudes as following $x_1 \to x_1 e^{-i\omega_m t} + x_1^* e^{i\omega_m t}$ and so on. We start with time domain equations for small amplitudes f_3 of symmetric mode and f_4 of anti-symmetric mode (see details in Appendix A):

$$\dot f_3(t) + \gamma_+ f_3(t) = \frac{-i\omega_1 N_1 \mathcal{F}_0}{L}\left(\zeta_+^* + x_{bs}^* + \sqrt{2}\, y_{pr}^*\right) e^{-i\Delta t}, \tag{2.1}$$

$$\gamma_+ = \frac{T_{pr}}{4\tau}, \quad \zeta_+ = \frac{2(x_1 + x_2) + (y_1 + y_2)}{\sqrt{2}}, \tag{2.2}$$

$$\Delta = \omega_0 - \omega_1 - \omega_m, \tag{2.3}$$

$$\dot f_4(t) + \Gamma_- f_4(t) = \frac{-\omega_1 N_1 \mathcal{F}_0}{L}\left(\zeta_-^* - x_{bs}^*\right) e^{-i\Delta t}, \tag{2.4}$$

$$\Gamma_- = \gamma_- - i\delta, \quad \gamma_- = \frac{T_{sr}}{4\tau}, \quad \delta = \frac{2\phi}{2\tau}, \tag{2.5}$$

$$\zeta_- = \frac{2(x_1 - x_2) + (y_1 - y_2)}{\sqrt{2}}. \tag{2.6}$$

Here γ_+, γ_- are relaxation rates of symmetric and anti-symmetric modes correspondingly. We assume that PR cavity is in resonance, i.e. phase advance ϕ_{pr} between beam splitter and PR mirror is fold to 2π: $\exp(i\phi_{pr}) = 1$. It means that mean amplitudes in SR cavity equal zero: $\mathcal{F}_4 = \mathcal{E}_4 = 0$. In contrast, we assume phase advance ϕ between beam splitter and SR mirror having an arbitrary value. We also assume that ϕ_{pr} (and ϕ) does not depend on time.

The coupling between Stokes and elastic mode arises as follows. The wave of main mode reflecting from surface of mirror, oscillating with frequency ω_m and having complex amplitude x, originates waves

$$\sim \left(F_0 e^{-i\omega_0 t} + F_0^* e^{i\omega_0 t}\right)\left(x e^{-i\omega_m t} + x^* e^{i\omega_m t}\right)$$

with frequencies $\omega_0 \pm \omega_m$. One of them (having frequency $\omega_0 - \omega_m$) is in resonance with Stokes mode — it is the origin of term in the right part of Eq. (2.1, 2.4). Another one (having frequency $\omega_0 + \omega_m$) is in resonance with anti-Stokes mode, which we do not take into account in our consideration.

Comparing left parts of Eqs. (2.1, 2.4) we see that resonance frequency of symmetric mode (ω_1) differs from resonance frequency of anti-symmetric mode by detuning δ which can be controlled by position of SR mirror.

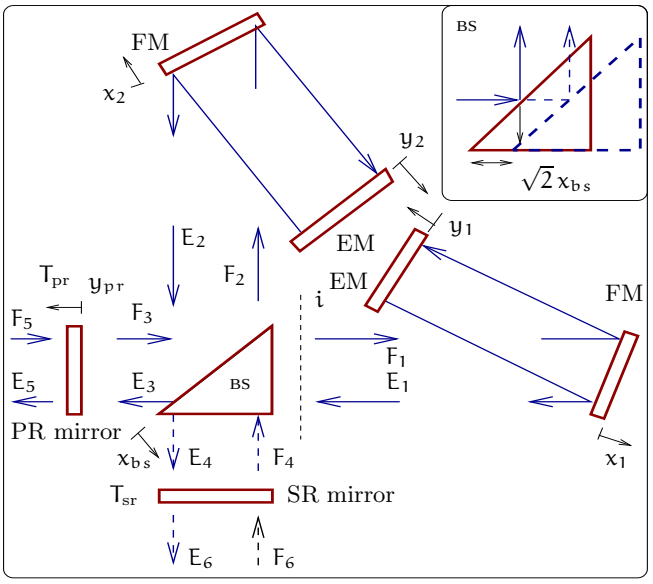

FIG. 1: Signal and power recycled GEO 600 interferometer. FM — folding mirrors, EM — end mirrors, BS — beam splitter. Here F_1, E_1 are amplitudes on plane (i), F_2, E_2, F_3, E_3, F_4, E_4 are amplitudes on beam splitter.

We have to supply Eqs. (2.1, 2.4) with equations for evolution of elastic mode amplitudes (see details in Appendix A):

$$\dot x_1^* + \gamma_m x_1^* = \frac{\sqrt{2}\, N_1^* \mathcal{F}_0^* (i f_3 - f_4) e^{i\Delta t}}{\omega_m m c\mu}, \tag{2.7}$$

$$\dot y_1^* + \gamma_m y_1^* = \frac{N_1^* \mathcal{F}_0^* (i f_3 - f_4) e^{i\Delta t}}{\sqrt{2}\omega_m m c\mu}, \tag{2.8}$$

$$\dot x_2^* + \gamma_m x_2^* = \frac{\sqrt{2}\, N_1^* \mathcal{F}_0^* (i f_3 + f_4) e^{i\Delta t}}{\omega_m m c\mu}, \tag{2.9}$$

$$\dot y_2^* + \gamma_m y_2^* = \frac{N_1^* \mathcal{F}_0^* (i f_3 + f_4) e^{i\Delta t}}{\sqrt{2}\omega_m m c\mu}, \tag{2.10}$$

$$\dot y_{pr}^* + \gamma_m y_{pr}^* = \frac{-N_1^* \sqrt{2}\mathcal{F}_0^* f_3 e^{i\Delta t}}{i\omega_m m_{pr} c\mu} \tag{2.11}$$

$$\dot x_{bs}^* + \gamma_m x_{bs}^* = \frac{N_1^* e^{i\Delta t} \mathcal{F}_0^* (i f_4 - f_3)}{i\omega_m m_{bs} c\mu}. \tag{2.12}$$

Here masses of folding and end mirrors in arms are denoted by m (they are equal to each other), m_{pr}, m_{bs} are masses of PR mirror and beam splitter correspondingly (elastic modes in SR mirror does not participate in parametric instability), ω_m, γ_m are normal frequency and relaxation rate of elastic mode, the other notations are given in Appendix A.

The waves of main and Stokes modes reflecting from the mirror produce radiation pressure force proportional to the square of sum field. In formula for this force we take into account the cross term only proportional to

$$\sim \left(\mathcal{F}_0 e^{-i\omega_0 t} + \mathcal{F}_0^* e^{i\omega_0 t}\right)\left(f_{Stokes} e^{-i\omega_1 t} + f_{Stokes}^* e^{i\omega_1 t}\right)$$

which contains the difference frequency $(\omega_0 - \omega_1)$ (in resonance with elastic mode). It originates the terms in the right parts of Eqs. (2.7 – 2.12).

TABLE I: Constants and parameters of GEO 600 used for estimates.

Symbol	Physical meaning	Numerical value
m	Masses of EM and FM	5.6 kg [21]
m_{pr}	Mass of PR mirror	2.9 kg [21]
m_{bs}	BS mirror mass	9.3 kg [21]
L	Effective arm length	1200 m
W	Light power circulating in each arm	planned 10 kW
ω_0	Mean frequency of carrier light	$1.8 \cdot 10^{15}$ s^{-1}
T_{pr}	Power transparency of PR mirror	0.09% [22]
γ_+	Relaxation rate of sym. mode	$\simeq 56$ s^{-1}
T_{sr}	Power transparency of SR mirror	1.9% [22]
γ_-	Relaxation rate of anti-sym. mode	$\simeq 1200$ s^{-1}
ω_m	Elastic mode frequency	$\simeq 10^6$ 1/sec
γ_m	Relaxation rate of elastic mode	$\simeq 0.125$ s^{-1}
ϕ_{loss}	Loss angle ($\gamma_m = \omega_m \phi_{loss}/2$)	2.5×10^{-7} [23]

B. Parametric instability conditions

The masses (and sizes) of end and folding mirrors (EM and FM) in arms of GEO 600 are practically the same, PR mirror and beam splitter have different masses (see Table I). Hence, there is a very small chance that frequencies and structures of elastic modes in beam splitter, PR and other mirrors (EM, FM) coincide, and we have to analyze parametric instability with elastic modes of these mirrors separately. Further, considering elastic modes in EM and FM we can assume that mirrors are elastically identical (i.e. the frequencies and structure of elastic modes are the same); then we can consider symmetric (subsec. II B 1) and anti-symmetric modes (subsec. II B 2). In the opposite case we can consider folding and end mirrors separately (subsec. II B 3), including PR mirror (subsec. II B 4) and beam splitter (subsec. II B 5). In subsec. II B 6 we present solution of characteristic equations obtained in subsec. II B 1 – II B 5.

For estimates we will use parameters of GEO 600 interferometer presented in Table I.

1. Symmetric mode

We see from equation (2.1) that amplitude f_3 depends on sum coordinate ζ_+ (recall that here we do not take into account dependence on coordinate x_{bs}, y_{pr} — it will be done below). Using Eqs. (2.7 – 2.10), we obtain the set of equations in time domain:

$$(\partial_t + \gamma_+)\, f_3(t) = \frac{-i\omega_1 N_1 \mathcal{F}_0}{L}\, \zeta_+^*\, e^{-i\Delta t}, \tag{2.13}$$

$$\dot\zeta_+^* + \gamma_m \zeta_+^* = \frac{5iN_1^* \mathcal{F}_0^* f_3 e^{i\Delta t}}{\omega_m m\, c\mu}\,. \tag{2.14}$$

We call this mode a symmetric one. Finding solution for this set as $f_3 = f_3 e^{\lambda t - i\Delta t}$, $\zeta_+ = \zeta_+ e^{\lambda t}$ we obtain characteristic equation (recall that optical power circulating in arms is equal to $|\mathcal{F}_0|^2 \equiv W$):

$$\frac{5\mathcal{Q}}{(\lambda+\gamma_m)(\lambda+\gamma_+ - i\Delta)} = 1, \tag{2.15}$$

$$\mathcal{Q} \equiv \frac{\omega_1 \Lambda W}{cLm\omega_m}, \quad \Lambda = \frac{|N_1|^2}{\mu} \tag{2.16}$$

Here Λ is overlapping factor (see also (A31)), it is equal to 1 if distribution of Stokes mode field and elastic mode displacement on mirror surface coincide completely, in reality $\Lambda < 1$. The parametric instability will takes place when the real part of one of the roots of this characteristic equation becomes positive.

2. Antisymmetric mode

For anti-symmetric mode we have similar set of equations in time domain, using (2.4) and (2.7 – 2.10):

$$\dot f_4 + \Gamma_- f_4 = \frac{-\omega_1 N_1 \mathcal{F}_0}{L}\, \zeta_-^*\, e^{-i\Delta t}, \tag{2.17}$$

$$\dot\zeta_-^* + \gamma_m \zeta_-^* = \frac{-5N_1^* \mathcal{F}_0^* f_4 e^{i\Delta t}}{\omega_m m\, c\mu} \tag{2.18}$$

Finding solution for this set as $f_4 = f_4 e^{\lambda t - i\Delta t}$, $\zeta_- = \zeta_- e^{\lambda t}$ we obtain characteristic equation:

$$\frac{5\mathcal{Q}}{(\lambda+\gamma_m)(\lambda+\Gamma_- - i\Delta)} = 1. \tag{2.19}$$

3. Single folding or end mirror

Now we can consider the case when only one mirror participates in parametric instability. This may happen when normal frequencies in different modes differ from each other by value $\Delta\omega_m$ larger than one of relaxation rates γ_+ or γ_- i.e. (using parameters from Table I) — $\Delta\omega_m/\omega_m \geq 10^{-3}$. Such difference may be easy produced by suspension system or caused by inhomogeneity of mirror material [10].

Considering, as an example, only folding mirror in east arm (position x_1) we obtain from Eqs. (2.1, 2.4, 2.7) the following set of equations:

$$(\partial_t + \gamma_+)\, f_3(t) = \frac{-i\sqrt{2}\omega_1 N_1 \mathcal{F}_0}{L}\, x_1^*\, e^{-i\Delta t}, \tag{2.20}$$

$$(\partial_t + \Gamma_-)\, f_4 = \frac{-\sqrt{2}\,\omega_1 N_1 \mathcal{F}_0}{L}\, x_1^* e^{-i\Delta t}, \tag{2.21}$$

$$\dot x_1^* + \gamma_m x_1^* = \frac{\sqrt{2}\, N_1^* \mathcal{F}_{l0}^* (if_3 - f_4) e^{i\Delta t}}{\omega_m m\, c\mu}, \tag{2.22}$$

Finding solution of this set as $f_3 = f_3 e^{\lambda t - i\Delta t}$, $f_4 = f_4 e^{\lambda t - i\Delta t}$, $x_1^* = x_1^* e^{\lambda t}$ we obtain characteristic equation:

$$\frac{2\mathcal{Q}}{\lambda+\gamma_m}\left(\frac{1}{\lambda+\gamma_+ - i\Delta} + \frac{1}{\lambda+\Gamma_- - i\Delta}\right) = 1\,. \tag{2.23}$$

We can obtain the same characteristic equation considering only the folding mirror in north arm (position x_2). Considering only one end mirror in any arm (positions y_1 or y_2) we obtain the same characteristic equation (2.23) but without factor 2 before $\mathcal{Q}$.

4. Single PR mirror

Considering only PR mirror (posision y_{pr}) one can obtain set of equations similar to Eqs. (2.13, 2.14) and characteristic equation similar to (2.15):

$$\frac{2\mathcal{Q}_{pr}}{(\lambda+\gamma_m)(\lambda+\gamma_+-i\Delta)}=1, \tag{2.24}$$

$$\mathcal{Q}_{pr}\equiv\frac{\omega_1\Lambda W}{cLm_{pr}\omega_m},\quad \Lambda=\frac{|N_1|^2}{\mu} \tag{2.25}$$

5. Single beam splitter

As a following example, we consider only the beam splitter — from Eqs. (2.1, 2.4, 2.12) we obtain

$$\partial_t f_3+\gamma_+ f_3(t)=\frac{-i\omega_1 N_1\mathcal{F}_0}{L}\,x^*_{bs}\,e^{-i\Delta t}, \tag{2.26}$$

$$\partial_t f_4+\Gamma_- f_4=\frac{\omega_1 N_1\mathcal{F}_0}{L}\,x^*_{bs}e^{-i\Delta t}, \tag{2.27}$$

$$\partial_t x^*_{bs}+\gamma_m x^*_{bs}=\frac{N_1^* e^{i\Delta t}\mathcal{F}_0^*(if_4-f_3)}{i\omega_m m_{bs}\,c\mu}. \tag{2.28}$$

Again, finding solution for this set as $f_3=f_3e^{\lambda t-i\Delta t}$, $f_4=f_4e^{\lambda t-i\Delta t}$, $x^*_{bs}=x^*_{bs}\,e^{\lambda t}$ we obtain the characteristic equation:

$$\frac{\mathcal{Q}_{bs}}{\lambda+\gamma_m}\left(\frac{1}{\lambda+\gamma_+-i\Delta}+\frac{1}{\lambda+\Gamma_--i\Delta}\right)=1\,, \tag{2.29}$$

$$\mathcal{Q}_{bs}\equiv\frac{\omega_1\Lambda W}{cLm_{bs}\omega_m},\quad \Lambda=\frac{|N_1|^2}{\mu}\,. \tag{2.30}$$

6. Solution of characteristic equations

Recall that parametric instability corresponds to the case when real part of one of the roots of characteristic equation becomes positive. The solution of characteristic equations can be considerably simplified if we take into account strong inequality (see parameters in Table I):

$$\gamma_m\ll\gamma_+,\ \gamma_- \tag{2.31}$$

This inequality allows us assuming that one of the roots which is interesting for us has imaginary part much less than relaxation rates γ_+, γ_- and we can find, for example for (2.15) an approximate solution and then the parametric instability condition:

$$\lambda\simeq-\gamma_m+\frac{5\mathcal{Q}}{\gamma_+-i\Delta},\ \Rightarrow\ \frac{5\mathcal{Q}}{\gamma_m}\,\mathrm{Re}\left(\frac{1}{\gamma_+-i\Delta}\right)\geq 1 \tag{2.32}$$

The characteristic equation (2.19) for anti-symmetric mode differs from corresponding equation (2.15) for symmetric mode only by Γ_- substituted instead of γ_+. Hence the parametric instability condition for anti-symmetric mode differs from (2.32) by the same substitution only. The same is true for characteristic equation (2.24) with substitution $2\mathcal{Q}_{pr}$ instead of $5\mathcal{Q}$ in (2.15).

Using the same consideration we obtain parametric condition from Eq. (2.23) (generalization for (2.29) is obvious):

$$\frac{2\mathcal{Q}}{\gamma_m}\,\mathrm{Re}\left(\frac{1}{\gamma_+-i\Delta}+\frac{1}{\Gamma_--i\Delta}\right)\geq 1\,. \tag{2.33}$$

To be on the safe side we solved numerically corresponding characteristic equations under assumption $\gamma_m/\gamma_\pm\leq 10^{-2}$ and checked that the approximations (2.32, 2.33) are valid with relative accuracy $<10^{-2}$.

III. DISCUSSION AND CONCLUSION

Looking at Eqs. (2.32, 2.33) we see that in case of zero detuning the parametric instability may take place in GEO 600 interferometer if factors $\mathcal{Q}/\gamma_m\gamma_\pm$ are greater than 1. For parameters from Table I we estimate:

$$\frac{\mathcal{Q}}{\gamma_m\gamma_+}\simeq 1.27\times\Lambda,\quad \frac{\mathcal{Q}}{\gamma_m\gamma_-}\simeq 0.06\times\Lambda, \tag{3.1}$$

$$\frac{\mathcal{Q}_{pr}}{\gamma_m\gamma_+}\simeq 2.45\times\Lambda. \tag{3.2}$$

Hence, one may conclude that chance to observe parametric instability in GEO 600 interferometer is small enough because (a) overlapping factor is usually small ($\Lambda<0.1$) and (b) detuning is non zero in reality and it will also depress parametric instability.

However, it would be very attractive to use GEO 600 as a testing area to develop and test methods of parametric instability suppression. For this purpose it is interesting to enhance parametric instability. Recall that symmetric mode is tuned in resonance with pump while anti-symmetric mode may be effectively detuned by displacement of SR mirror. Owing to this detuning one can easy obtain the information on the frequencies and structures of elastic modes through observing signal at the output port (using balance homodyne detector not shown on Fig. 1) peaks of elastic oscillations in mirrors. This detuning can be done in range (part of free spectral range: $\Delta f_{frs}\simeq 600$ Hz) large enough to scan the range of elastic frequencies (50 ... 300 Hz) interesting for us. Therefore, one can choose a suitable elastic mode (i.e. overlapping factor Λ is not small) and tune antisymmetric mode in resonance (i.e. $\Delta\simeq 0$).

Now in order to observe parametric instability we have either to increase the optical power circulating in arms or to decrease relaxation rate γ_- of anti-symmetric mode by approximately two orders. Increasing optical power poses a difficult problem. Replacement of SR mirror by another one having smaller transparency in operating interferometer is undesirable. However, effective manipulation by SR mirror transparency can be done in another manner. One can place another mirror with transparency $T_{add}\simeq 0.01$ parallel to SR mirror so that these mirrors assemble a short Fabry-Perot cavity. Such replacement of SR mirror by additional 'SR' cavity was discussed in [24]. The transparency of this cavity vary from $4T_{sr}T_{add}/(T_{sr}+T_{add})^2$ (resonance) to $T_{sr}T_{add}/4$ (anti-resonance) by displacement of additional mirror. So tuning additional Fabry-Perot cavity close to anti-resonance one can decrease effective transparency of SR mirror by several orders. Note that additional mirror may be placed outside of the vacuum system of interferometer. It may provide additional noise but it is no barrier to PI observation.

Observation of parametric instability and its precursors in GEO 600 interferometer (in spite of it is not planned now) will provide the best approach to explore this phenomenon, develop experimental methods to depress it and to test effectiveness of these methods *in situ*.

Acknowledgments

We are grateful to Vladimir Braginsky, Bill Kells and David Ottaway for useful discussions on parametric instability problem. Especially we would like to thank Hartmut Grote, as fruitful discussions with him stimulated us to write this paper and Stefan Hild who provided us with valuable information on GEO 600 parameters. This work was supported by LIGO team from Caltech and in part by NSF and Caltech grant PHY-0353775, by the Russian Agency of Industry and Science: contract No. 5178.2006.2.

Appendix A: Derivation of main formulas

The electric field E in traveling wave, for example, in right arm of GEO 600 interferometer and mean power W is written as following:

$$\begin{aligned}
&E(t,\vec{r}_\perp) \simeq \sqrt{\frac{2\pi}{cS_0}}\mathcal{A}_0(\vec{r}_\perp)\mathcal{F}_0 e^{-i\omega_0 t} + \\
&+\sum_n \sqrt{\frac{2\pi}{cS_1^{(n)}}}\int_{-\infty}^{\infty}\mathcal{A}_1^{(n)}(\vec{r}_\perp)f_1^{(n)}(\Omega)e^{-i(\omega_1+\Omega)t}\frac{d\Omega}{2\pi} + \\
&\quad + \text{h.c.}, \\
&W = \left|\mathcal{F}_0\right|^2, \\
&S_0 = \int_S |\mathcal{A}_0(\vec{r}_\perp)|^2\, d\vec{r}_\perp, \quad S_1^{(n)} = \int_S |\mathcal{A}_1^{(n)}(\vec{r}_\perp)|^2\, d\vec{r}_\perp\,.
\end{aligned}$$

Here W is the mean power in traveling wave of main mode, dimensionless functions $\mathcal{A}_0(\vec{r}_\perp)$, $\mathcal{A}_1^{(n)}(\vec{r}_\perp)$ describe the distributions of optical fields over cross section for main and other (Stokes) modes, integration $\int_S d\vec{r}_\perp$ is taken over the mirror surface.

The Stokes wave appears after each reflection of the main wave from mirror surface oscillating with frequency ω_m. For example, we have for reflection from mirror with position x_1:

$$\begin{aligned}
\sum_n \frac{\mathcal{A}_1^{(n)}}{\sqrt{S_1^{(n)}}}\, e_1^{(n)} e^{-i\omega_1 t} = -\sum_n \frac{\mathcal{A}_1^{(n)}}{\sqrt{S_1^{(n)}}}\, f_1^{(n)} e^{-i\omega_1 t} - \\
- \frac{\mathcal{A}_0}{\sqrt{S_0}}\,\mathcal{F}_0 e^{-i\omega_0 t}\, 2ik u_\perp \left(x_1 e^{-i\omega_m t} + x_1^* e^{i\omega_m t}\right).
\end{aligned}$$

Here sum is taken over complete set $\mathcal{A}_1^{(n)}$ of cavity modes (they are orthogonal to each other) and $u_\perp$ is normal to surface component of dimensionless displacement vector $\vec{u}$ of elastic mode and x_1 is slow amplitude of displacement, $k = \omega_1/c$. Multiplying this equation by distribution function $\mathcal{A}_1^*/\sqrt{S_1}$ of more suitable Stokes mode (we drop index $^{(n)}$ from this point on), integrating over cross section and omitting non-resonance term ($\sim x_1 e^{-i\omega_m t}$) one can obtain in the frequency domain:

$$e_1(\Omega) = -f_1(\Omega) - N_1\mathcal{F}_{0in}\, 2ik x_1^*(\Delta-\Omega), \tag{A1}$$

$$N_1 = \frac{\int_S \mathcal{A}_0\mathcal{A}_1^*\, u_\perp(\vec{r})\, d\vec{r}_\perp}{\sqrt{\int_S |\mathcal{A}_0|^2\, d\vec{r}_\perp \int_S |\mathcal{A}_1|^2\, d\vec{r}_\perp}}, \tag{A2}$$

$$\Delta = \omega_0 - \omega_1 - \omega_m.$$

Below we apply these consideration to each reflection. However, for simplicity we do not write factor N_1 in every formula and restore it in final formulas (after expanding exponents like e^{ikx} in series).

Beam Splitter. We consider that F_2, E_2, F_3, E_3, F_4, E_4 are amplitudes on beam splitter (its transparency is equal to $T_{bs} = 1/2$) as shown in Fig. 1. Amplitudes F_1, E_1 we consider on plane (i) (see Fig. 1) so that phase advance between beam splitter and this plane is $e^{i\phi_1} = i$. F_2, E_2 are amplitudes on beam splitter. The phase $\phi_{bs} = \sqrt{2}\,k x_{bs}$ is introduced due to shifting position x_{bs} of the beam splitter. Thus, we have:

$$\frac{F_1}{i} = \frac{iF_3 - F_4 e^{-i\phi_{bs}}}{\sqrt{2}}, \quad F_2 = \frac{1}{\sqrt{2}}\left(-F_3 e^{i\phi_{bs}} + iF_4\right), \tag{A3}$$

$$E_3 = \frac{i(i)E_1 - E_2 e^{i\phi_{bs}}}{\sqrt{2}}, \quad E_4 = \frac{i\left(-E_1 e^{-i\phi_{bs}} + E_2\right)}{\sqrt{2}}. \tag{A4}$$

Arms. Denoting $\tau = L/c$ where L is the path length between the beam splitter and the end mirror in each arm, we have:

$$E_1 = -\theta F_1 e^{2ikz_1}, \quad E_2 = -\theta F_2 e^{2ikz_2}, \tag{A5}$$

$$\theta = e^{2i\Omega\tau} \simeq 1 + 2i\Omega\tau, \quad z_{1,2} = 2x_{1,2} + y_{1,2} \tag{A6}$$

Substituting (A5, A3) into (A4) we obtain:

$$\begin{aligned}
E_3 = \frac{-\theta F_3}{2}\left(e^{2ikz_1} + e^{2ikz_2 + 2i\phi_{bs}}\right) + \\
+ \frac{iF_4\theta}{2}\left(-e^{2ikz_1 - i\phi_{bs}} + e^{2ikz_2 + i\phi_{bs}}\right),
\end{aligned} \tag{A7}$$

$$\begin{aligned}
E_4 = \frac{\theta i F_3}{2}\left(-e^{2ikz_1 - i\phi_{bs}} + e^{2ikz_2 + i\phi_{bs}}\right) + \\
+ \frac{\theta F_4}{2}\left(e^{2ikz_1 - 2i\phi_{bs}} + e^{2ikz_2}\right)
\end{aligned} \tag{A8}$$

We consider the case when PR cavity is in resonance (see below) — this means that the mean amplitude $\mathcal{F}_4 = 0$. Hence, as it follows from (A3) that the mean amplitudes in arms are equal to each other and we denote them by $\mathcal{F}_0$ (i.e. $\mathcal{F}_1 = \mathcal{F}_2 = \mathcal{F}_0$). Then we can obtain the formulas for mean amplitudes:

$$\mathcal{F}_1 = \mathcal{F}_2 = \frac{-\mathcal{F}_3}{\sqrt{2}} = \mathcal{F}_0, \quad \mathcal{E}_1 = \mathcal{E}_2 = \frac{\mathcal{F}_3}{\sqrt{2}} = -\mathcal{F}_0, \tag{A9}$$

$$\mathcal{F}_3 = \frac{-\mathcal{F}_1 - \mathcal{F}_2}{\sqrt{2}} = -\sqrt{2}\,\mathcal{F}_0, \quad \mathcal{E}_3 = \sqrt{2}\,\mathcal{F}_0, \quad \mathcal{F}_4 = 0. \tag{A10}$$

From Eqs. (A7, A8) expanding exponents in series and restoring factor N_1 like in (A1) we obtain for small amplitudes

$$e_3(\Omega) = -\theta f_3(\Omega) + N_1\mathcal{F}_0\, 2ik\left(\zeta_+^*(\Delta-\Omega) + x_{bs}^*(\Delta-\Omega)\right), \tag{A11}$$

$$e_4(\Omega) = \theta\, f_4(\Omega) + iN_1\mathcal{F}_0 2ik\left(\zeta_-^*(\Delta-\Omega) - x_{bs}^*(\Delta-\Omega)\right), \tag{A12}$$

$$\zeta_+ = \frac{z_1+z_2}{\sqrt{2}}, \quad \zeta_- = \frac{z_1-z_2}{\sqrt{2}} \tag{A13}$$

For Power Recycling Mirror we have:

$$F_3 e^{-i\phi_{pr}} = i\sqrt{T_{pr}}F_5 - \sqrt{1-T_{pr}}E_3 e^{i\phi_{pr}}(1+2iky^*_{pr}), \tag{A14}$$

$$\phi_{pr} = (\omega_1 + \Delta_{pr} + \Omega)l_{pr}/c. \tag{A15}$$

Here last term in brackets in the right side of (A14) corresponds to expansion in series of term $e^{2iky_{pr}}$. We assume that PR cavity is in resonance, i.e. $\exp(i\phi_{pr}) = 1$ and ϕ_{pr} does not depend on frequency Ω due to shortness of PR cavity. Below we use for small amplitude only Eq. (A14) omitting term $\sim F_5$ (because there is no pumping of Stokes mode):

$$f_3 = -\sqrt{1-T_{pr}}e_3 - \sqrt{1-T_{pr}}N_1\mathcal{E}_3\, 2iky^*_{pr}. \tag{A16}$$

And substituting (A11) into (A16) we get:

$$f_3(1-\theta\sqrt{1-T_{pr}}) = -\sqrt{1-T_{pr}}\,N_1\mathcal{F}_0\times \times 2ik(\zeta^*_+ + x^*_{bs} + \sqrt{2}y^*_{pr}). \tag{A17}$$

Expanding in series $e^{2i\Omega\tau} \simeq 1 + 2i\Omega\tau$, $\sqrt{1-T_{pr}} \simeq 1 - T_{pr}/2$ in Eq. (A17) we can obtain in frequency domain:

$$f_3(\gamma_+ - i\Omega) = \frac{-i\omega_1 N_1\mathcal{F}_0(\zeta^*_+ + \sqrt{2}\,y_{pr} + x^*_{bs})}{L}, \tag{A18}$$

$$\zeta_+ = \frac{2(x_1+x_2)+(y_1+y_2)}{\sqrt{2}}, \quad \gamma_+ = \frac{T_{pr}}{4\tau}. \tag{A19}$$

Now using obvious rule $(-i\Omega) \Rightarrow \partial_t$ one can obtain Eq. (2.1) in time domain from Eq. (A18).

For Signal Recycling Mirror we have:

$$F_4 e^{-i\phi} = i\sqrt{T_{sr}}F_6 - \sqrt{1-T_{sr}}E_4 e^{i\phi}. \tag{A20}$$

We assume that SR cavity is not in resonance (i.e. the phase advance ϕ between beam splitter and SR mirror has an arbitrary value) and we also assume that ϕ does not depend on frequency Ω. Again for small amplitudes we omit term $\sim F_6$ in Eq. (A20)

$$f_4 + \sqrt{1-T_{sr}}e^{i2\phi}\, e_4 = 0. \tag{A21}$$

Now substituting (A12) into (A21) we get:

$$f_4(1+\theta e^{2i\phi}\sqrt{1-T_{sr}}) = -iN_1\mathcal{F}_0 e^{2i\phi}\sqrt{1-T_{sr}}\times \times 2ik(\zeta^*_- - x^*_{bs}). \tag{A22}$$

Below we assume convention: $\phi \to \phi + \pi/2$ (it corresponds to resonance for anti-symmetric mode is $\phi = 0$):

$$f_4(1-\theta e^{2i\phi}\sqrt{1-T_{sr}}) = +iN_1\mathcal{F}_0 e^{2i\phi}\sqrt{1-T_{sr}}\times \times 2ik(\zeta^*_- - x^*_{bs}). \tag{A23}$$

Expanding in series $e^{2i\Omega\tau} \simeq 1 + i2\Omega\tau$, $e^{2i\phi} \simeq 1 + 2i\phi$, $\sqrt{1-T_{sr}} \simeq 1 - T_{sr}/2$ in Eq. (A23) we can obtain in frequency domain:

$$f_4(\Gamma_- - i\Omega) = \frac{-\omega_1 N_1\mathcal{F}_0}{L}(\zeta^*_- - x^*_{bs}), \tag{A24}$$

$$\Gamma_- = \gamma_- - i\delta, \quad \gamma_- = \frac{T_{sr}}{4\tau}, \quad \delta = \frac{2i\phi}{2\tau}. \tag{A25}$$

Now one can obtain time domain Eq. (2.4) from Eq. (A24) using rule $(-i\Omega) \Rightarrow \partial_t$.

Ponderomotive forces. Considering the end mirror with coordinate y_1 we substitute the light pressure force acting on it into equation for the mirror coordinate y_1:

$$F_{y1} = \frac{2}{c}\left(N_1\mathcal{F}_0 f_1^* e^{-i(\omega_0-\omega_1)t} + N_1^*\mathcal{F}_0^* f_1\, e^{i(\omega_0-\omega_1)t}\right), \tag{A26}$$

$$\ddot{y}_1 + \gamma_m\dot{y}_1 + \omega_m^2 y_1 = \frac{F_{y1}}{m\mu}, \tag{A27}$$

$$\mu = \frac{\int_V |\vec{u}(\vec{r})|^2\, d\vec{r}}{V}, \tag{A28}$$

where integration is taken over volume V of mirror. Presenting $y_1 \to y_1 e^{-i\omega_m t} + y_1^* e^{i\omega_m t}$ we finally find equation (2.8) for slow amplitude y_1^* using (A3) and similar equation (2.7) for x_1^* (the force acting on mirror with coordinate x_1^* is two times larger). The equations (2.9, 2.10, 2.11) can be obtained in a similar way.

For the slow amplitudes x_{bs} of beam splitter we have:

$$\dot{x}^*_{bs} + \gamma_m x^*_{bs} = \frac{N_1^* e^{i\Delta t}}{2i\omega_m m_{bs}\, c\mu} \times \frac{G}{\sqrt{2}}, \tag{A29}$$

$$G \equiv \left(\mathcal{F}_3^* f_3 + \mathcal{F}_2^* f_2 - \mathcal{F}_1^* f_1 + \mathcal{E}_3^* e_3 + \mathcal{E}_2^* e_2 - \mathcal{E}_1^* e_1\right),$$

simplify using (A3, A9) :

$$G = \mathcal{F}_0^*\left(-f_1 + f_2 + e_1 - e_2 - \sqrt{2}(f_3 - e_3)\right) \simeq$$

$$\simeq \mathcal{F}_0^*(2\sqrt{2}\,if_4 - 2\sqrt{2}f_3) =$$

$$= 2\sqrt{2}\,\mathcal{F}_0^*(if_4 - f_3) = 4\mathcal{F}_0^* f_2. \tag{A30}$$

In the right part of equation (A29) factor 2 in denominator of the first multiplier appears when we go to equation for slow amplitudes (absence of factor 2 in numerator in contrast to (A26) is due to our taking into account both incident and reflecting waves in term G), and factor $\sqrt{2}$ in denominator of the second multiplier is due to accounting for only projection on axis x_{bs}. As a result we find equation (2.12) for slow amplitude x_{bs}.

The overlapping factor Λ is equal to (see Eqs.(A2, A28)):

$$\Lambda \equiv \frac{|N_1|^2}{\mu} = \frac{V\left|\int_S \mathcal{A}_0\mathcal{A}_1^*\, u_\perp(\vec{r})\, d\vec{r}_\perp\right|^2}{\int_S |\mathcal{A}_0|^2\, d\vec{r}_\perp \int_S |\mathcal{A}_1|^2\, d\vec{r}_\perp \int_V |\vec{u}(\vec{r})|^2\, d\vec{r}} \tag{A31}$$

[1] A. Abramovici *et al.*, *Science* **256**, 325 (1992).

[2] A. Abramovici *et al.*, *Physics Letters* **A218**, 157 (1996).

[3] LIGO technical document G060052-00-E; current sensitivity curves are available on http://www.ligo.caltech.edu/ lazz/ distribution/LSC_Data/ .
[4] Advanced LIGO System Design (LIGO-T010075-00-D), Advanced LIGO System requirements (LIGO-G010242-00), available in http://www.ligo.caltech.edu .
[5] http://www.ligo.caltech.edu/~ligo2/scripts/ 12refdes.htm
[6] http://www.geo600.uni-hannover.de/geocurves
[7] S. Hild, *Class. Quantum Grav.* **23**, S643-S651 (2006)
[8] V. B. Braginsky, S. E. Strigin, and S. P. Vyatchanin, *Physics Letters* **A287**, 331 (2001); gr-qc/0107079.
[9] E. D'Ambrosio and W. Kells, *Physics Letter* **A299**, 326 (2002). LIGO-T020008-00-D, available in http://www.ligo.caltech.edu.
[10] V. B. Braginsky, S. E. Strigin and S. P. Vyatchanin, *Physics Letters* **A305**, 111 (2002).
[11] A.G. Gurkovsky, S.E. Strigin and S. P. Vyatchanin, *Physics Letters* **A362**, 91-99 (2007); arXive: gr-qc/0608007.
[12] S.E. Strigin and S.P. Vyatchanin, accepted for publication in *Physics Letters A*; available in http://www.ligo.caltech.edu .
[13] V. B. Braginsky and S. P. Vyatchanin, *Physics Letters* **A293**, 228 (2002).
[14] C. Zhao, L. Ju, J. Degallaix, S. Gras, and D. G. Blair, *Phys. Rev. Lett.* **94**, 121102 (2005).
[15] L. Ju, S. Gras, C. Zhao, J. Degallaix and D. G. Blair, *Physics Letters* **A354**, 360 (2006).
[16] L. Ju, C. Zhao, S. Gras, J. Degallaix, D. G. Blair, J. Munch and D. H. Reitze, *Physics Letters* A, accepted (2006).
[17] T. Corbitt, D. Ottaway, E. Innerhofer, J. Pelc, and N. Mavalvala *Phys. Rev.* **A 74**, 021802 (2006).
[18] T. J. Kippenberg, H. Rokhsari, T. Carmon, A. Scherer, and K. J. Vahala, *Phys. Rev. Lett.* **95**, 033901, July 2005.
[19] H. Rokhsari, T. J. Kippenberg, T. Carmon, and K. J. Vahala, Optics express **13**, 5293 (2005).
[20] S.E. Strigin and S.P. Vyatchanin, *Physics Letters* **A365**, 10 - 16 (2007).
[21] S. Goβler, Ph.D. Thesis, Hannover University (2004).
[22] S. Hild, Ph.D. Thesis, Hannover university (2007).
[23] J. R. Smith, G. Cagnoli, D. R. M. Crooks, M. M. Fejer, S Goβler, H. Lück, S. Rowan, J. Hough and K. Danzmann *Class. Quantum Grav.*, S1091-S1098 (2004).
[24] S. Hild, available in http://www.ligo.caltech.edu/docs/G/G060342-00/G060342-00.pdf